Elsevier Editorial System(tm) for Carbohydrate Polymers

Manuscript Draft

Manuscript Number: CARBPOL-D-19-01342R1

Title: Combined effect of cellulose nanocrystals, carvacrol and oligomeric lactic acid in PLA_PHB polymeric films

Article Type: Research Paper

Keywords: Poly(lactic acid); Cellulose nanocrystals; Plasticizer; Nanocomposites; Compost disintegrability; Enzymatic degradation.

Corresponding Author: Dr. Ilaria Armentano,

Corresponding Author's Institution: Tuscia University

First Author: Francesca Luzi

Order of Authors: Francesca Luzi; Franco Dominici; Ilaria Armentano; Elena Fortunati; Nuria Burgos; Stefano Fiori; Alfonso Jimenez; Josè M Kenny; Luigi Torre

Abstract: Biodegradable multicomponent films based on poly(lactic acid) (PLA) and poly(3-hydroxybutyrate) (PHB) plasticized with oligomeric lactic acid (OLA), reinforced with synthetized cellulose nanocrystals (CNC) and modified by a natural additive with antimicrobial activity (carvacrol) were formulated and processed by extrusion. Morphological, mechanical, thermal, migration and barrier properties were tested to determine the effect of different components in comparison with neat poly(lactic acid). Results showed the positive effect of CNC in the five components based films, with the increase of the Young's modulus of the PLA_PHB_10Carv_15OLA, associated with an increase in the elongation at break (from 130% to 410%), by showing an OTR reduction of 67%. Disintegrability in compost conditions and enzymatic degradation were tested to evaluate the post-use of these films. All formulations disintegrated in less than 17 days, while proteinase K preferentially degraded the amorphous regions, and crystallinity degree of the nanocomposite films increased as a consequence of enzyme action.

HIGHLIGHTS

-PLA_PHB blend films with OLA, antibacterial additive and CNC were developed

-OLA as natural plasticizer into the blend improves the ductile properties

-CNC introduction improves film barrier properties

-CNC in the five component film increase the Young modulus and the elongation at break.

-All formulations disintegrated in composting conditions in less than 17 days

GRAPHICAL ABSTRACT

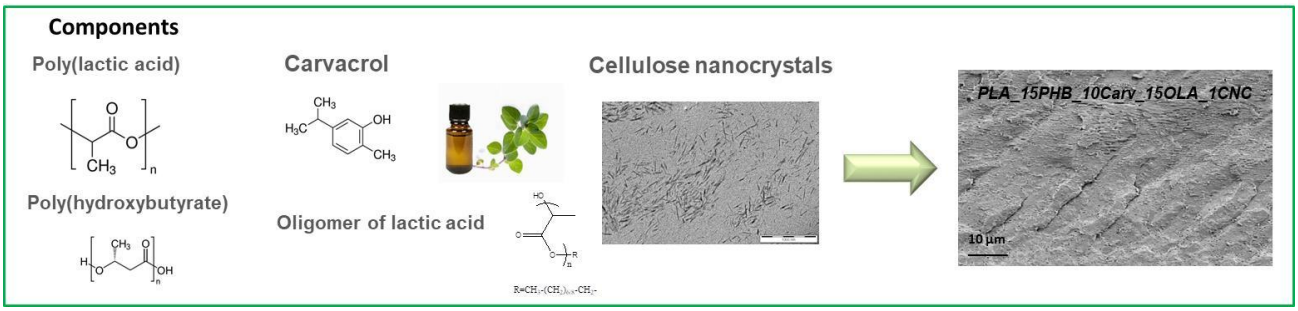

ABSTRACT

Biodegradable multicomponent films based on poly(lactic acid) (PLA) and poly(3-hydroxybutyrate) (PHB) plasticized with oligomeric lactic acid (OLA), reinforced with synthetized cellulose nanocrystals (CNC) and modified by a natural additive with antimicrobial activity (carvacrol) were formulated and processed by extrusion. Morphological, mechanical, thermal, migration and barrier properties were tested to determine the effect of different components in comparison with neat poly(lactic acid). Results showed the positive effect of CNC in the five components based films, with the increase of the Young's modulus of the PLA_PHB_10Carv_15OLA, associated with an increase in the elongation at break (from 130% to 410%), by showing an OTR reduction of 67%. Disintegrability in compost conditions and enzymatic degradation were tested to evaluate the post-use of these films. All formulations disintegrated in less than 17 days, while proteinase K preferentially degraded the amorphous regions, and crystallinity degree of the nanocomposite films increased as a consequence of enzyme action.

KEYWORDS: Poly(lactic acid); Cellulose nanocrystals; Plasticizer; Nanocomposites; Compost disintegrability; Enzymatic degradation

1. INTRODUCTION

The growing demand for safe food, the prevention of human health from food contamination and the great environmental concerns raised in the last decade have directed attention to develop and design new, green, biodegradable and active food packaging systems, where multifunctional sustainable materials could be formulated for such purpose (Atares & Chiralt, 2004; Arrieta, López, Hernández, & Rayón, 2014; Valdés, Mellinas, Ramos, Garrigós, & Jiménez, 2014; Cano, Cháfer, Chiralt, & González-Martínez, 2015). The introduction of green and eco-friendly products on the global market represents a valid and strategic possibility to reduce the high quantities of wastes accumulated on the landfill and to substitute environmentally deleterious petrochemical-based plastics (Luzi, et a., 2016; Avarez-Chavez, Edwards, Moure-Eraso & Geiser, 2012). In this context, the food packaging sector can be considered as a major area for the introduction of bio-based and biodegradable materials, since their environmental impact can be limited when compared to conventional packaging materials (Mlalila, Hilonga, Swai, Devlieghere & Ragaert, 2018; Youssef & El-Sayed, 2018; Armentano, et al., 2015a).

Poly(lactic acid) (PLA) is the most popular and investigated biopolymer since it can be used in short-term and disposable products, such as bottles, bags, films and disposable cutlery (Armentano, et al, 2013; Martino, Jimenez, Ruseckaite & Aveorus, 2011; Habibi, Aouadi, Raquez, & Dubois, 2013) as well as in flexible and rigid food packaging applications (Boonyawan, et al., 2011); PLA has been approved by the US Food and Drug Administration

(FDA) for direct contact with food, showing high transparency and easy processability. However, PLA presents also some limitations in these applications, such as poor oxygen and water vapour barrier (necessary for fresh food packaging), as well as low thermal and mechanical properties (Fortunati, et al., 2012).

Developing PLA-based multifunctional systems, in which materials with complementary properties are mixed in the same formulation in a combined way, could be an interesting approach to overcome these shortcomings. In particular the introduction of nanomaterials in plasticized biopolymeric blends has been considered as a strategic opportunity to modulate the functional and final characteristics of PLA (Habibi, Aouadi, Raquez, & Dubois, 2013; Fortunati, et al., 2014; Arrieta, et al., 2014). Following this strategy, poly(3-hydroxybutyrate) (PHB), a microorganism-synthesized aliphatic polyester with high crystallinity and melting point can be selected and combined with PLA to improve thermal, mechanical, barrier and physical properties, as it has been already reported in previous work from our research group (Armentano, et al., 2015; Arrieta, et al. 2014b, Armentano, et al., 2015b; Arrieta, et al., 2014b; Arrieta, Samper, Aldas, & Lopez, 2017).

Cellulose nanocrystals (CNC) have been also considered as interesting ecofriendly solutions to tune the properties of biodegradable polymers (Valdés, Mellinas, Ramos, Garrigós, & Jiménez, 2014; Zhu, et al., 2018). CNC are extracted from different sources in the form of rigid-rod monocrystalline domains with diameters ranging from 1-100 nm and from tens to hundreds of nm in length (Ruiz, Cavaille, Dufresne, Gerard, & Graillat, 2000), depending on the sources and applied procedures for their extraction (Cranston & Gray, 2006; Luzi, et al., 2016). Another potential strategy to improve the properties of PLA is by the use of plasticizers (Fortunati, et al., 2014; Burgos, Martino & Jimenez, 2013; Arrieta, Fortunati, Dominici, Lopez, Kenny, 2015). We

have proposed to increase the ductility and the processability of PLA by using oligomeric lactic acid (OLA), a bio-based plasticizer able to improve elongation at break (Armentano, et al., 2015b; Burgos, Martino, & Jimenez, 2013) so, to increase the plastic behavior of the obtained biocomposites. Here the main aim of this research paper is to show the development of innovative packaging materials based on fully sustainable and biodegradable components, by combining biopolymers already used in industrial packaging (polylactic acid (PLA), polyhydroxybutyrates (PHB)), bio-based plasticizers, natural additives with bio-based nanofillers, with the aim to develop multifunctional, cost-effective, and sustainable nanocomposites. One of the main interests of the research is to minimize the PLA and PHB current limitations for packaging applications such as low thermal resistance and flexibility, water permeability, difficult processability, and insufficient food protection. The addition of specific and innovative reinforcing materials such as cellulose nanocrystals, antimicrobians and biodegradable plasticizers identified within the scientific research will resolve these inconvenients. Furthermore the analysis of the combination of the different additives, an optimum choice of their ratio, and processing parameters led to high performance biodegradable materials. The main novelty of this research work deal in the successfully development of new bio-based films by a combination of five different components, that all came from renewable resources. Previous studies have shown the development of PLA_PHB plasticized blend, reinforced with CNC, but without the addition of a bio-based antibacterial agent, and selecting ATBC as plasticizer (Arrieta, Fortunati, Dominici, Lopez, & Kenny, 2015). Recently Seoane et al., compares the behavior of nanocomposites made with two different plasticizers and two types of nanocellulose (Seoane, Cerrutti, Vasquez, Cyras & Manfredi, 2019). However we did not find published papers with five different components, based on PLA polymer matrix.

This work represents the final step of a research project in which we have combined PLA with different green additives and materials in order to improve its final properties. In particular, this research proposes the combination of PLA with PHB (15 wt%), plasticized with an OLA in two different concentrations (15 and 30 wt%), in the presence of a natural active ingredient (carvacrol) (10 wt%) and CNC (1 and 3 wt%) extracted from commercial microcrystalline cellulose (MCC). The produced films were investigated and characterized in terms of thermal, morphological, mechanical and barrier properties. The overall migration study was carried out by using two different food simulants to evaluate the effect of additives diffusion into the polymer matrix, whereas disintegrability in composting conditions and enzymatic degradation were tested to evaluate the post-use possibilities of these systems.

2. Experimental

2.1. Materials.

Poly(lactic acid) (PLA3051D) was purchased from NatureWorks® Co. LLC (USA). This PLA grade is characterized by a molecular weight (Mn) of 1.42×10^4 g mol^{-1}, specific gravity of 1.25 g cm^{-3} and melt flow index (MFI) of 7.75 g/10min tested at 210 °C and 2.16 kg loading. Poly(3-hydroxybutyrate) (PHB), supplied by NaturePlast (Caen, France), has a density of 1.25 g cm^{-3}, MFI 15-30 g /10 min tested at 190 °C and 2.16 kg loading. The lactic acid oligomer (OLA) (Mn 957 g mol^{-1} and glass transition temperature around -37 ºC) was selected as plasticizer and was supplied by Condensia Quimica S.A (Barcelona, Spain). Three different OLAs were considered in our studies and the selection was due according to specific physical and chemical properties, (viscosity, thermal stability). (Burgos, Tolaguera, Fiori & Jimenez, 2013) Carvacrol (Carv, > 98% purity) was purchased from Sigma-Aldrich (Madrid, Spain). Cellulose nanocrystals were

obtained by acidic hydrolysis as previously reported (Luzi, et al., 2014; Fortunati, et al., 2013) by using microcrystalline cellulose (MCC, dimensions 10–15 μm; Sigma–Aldrich®) as raw material. The obtained CNC showed individualized crystal domains 5-10 nm in width and 100-200 nm in length (Fortunati, et al., 2013; Fortunati, et al., 2017), Their final dry-content in aqueous solution was around 0.4 (wt/wt) % and the reaction yield was about 20 %.

2.2. Processing

PLA and PLA_15PHB-based multifunctional systems loaded with OLA and/or carvacrol and reinforced with CNC were processed by using a twin-screw microextruder (DSM Xplore 15 CC Micro Compounder). PLA, PHB and CNC were pre-dried to avoid any moisture trace and undesirable hydrolysis reactions during processing. PLA was oven-heated at 98 °C for 3 h, PHB was dried at 70 °C for 4 h, while CNC were dried at 40 °C for 12 h. Finally, OLA was heated for 5 min at 100 °C to facilitate the mixing procedure into the microextruder. PLA_PHB blends were obtained by addition of PHB at 15 wt% to a PLA matrix on the basis of our previous work (Armentano, et al., 2015b) and were reinforced with 1 wt% and 3 wt% of CNC (Arrieta, et al., 2014c). Then, the effect of OLA as plasticizer in the selected formulation (reinforced with 1 wt% CNC) was evaluated. Finally, the combined effect of carvacrol with OLA in the PLA_PHB blends was addressed in the case of PLA_15PHB_15OLA_10Carv_1CNC multifunctional five-components formulation. The content of CNC in this formulation was selected on the basis of thermal and mechanical characterization of ternary and four-components systems, while the content of OLA was reduced to 15 wt% to consider the combined effect of two agents able to induce plasticization (lactic oligomer and carvacrol) (Armentano et al. 2015). **Table 1** shows the component's contents and the mixing parameters to produce different multifunctional formulations. Films with thicknesses ranging between 20 and 60 μm were obtained by extrusion

process, with the adequate filming tip. The temperature profile was set up at 180-190-200 ºC in the three different extruder areas, the screw speed was fixed at 100 rpm, while the time for the mixing process was established at 6 min, as reported in **Table 1**.

Table 1. Material formulations and process parameters.

Formulations	Component contents					Mixing parameters		
	PLA (wt%)	PHB (wt%)	OLA (wt%)	CNC (wt%)	Carv (wt%)	Speed (rpm)	Mixing time (min)	Temperature Profile (°C)
PLA	100	-	-	-	-	100	6	180-190-200
PLA_15PHB	85	15	-	-	-	100	6*	180-190-200
PLA_15PHB_CNC films								
PLA_15PHB_1CNC	84	15	-	1	-	100	6*	180-190-200
PLA_15PHB_3CNC	82	15	-	3	-	100	6*	180-190-200
PLA_15PHB_30OLA films								
PLA_15PHB_30OLA	55	15	30	-	-	100	6**	180-190-200
PLA_15PHB_30OLA_1CNC	54	15	30	1	-	100	6**	180-190-200
PLA_15PHB_15OLA_10Carv films								
PLA_15PHB_15OLA_10Carv	60	15	15	-	10	100	6**	180-190-200
PLA_15PHB_15OLA_10Carv_1CNC	59	15	15	1	10	100	6**	180-190-200

*PLA mixed 6 min, PHB mixed last 3 min, CNC mixed last 2 min

**PLA_PHB mixed 6 min, OLA and/or Carv mixed last 3 min, CNC mixed last 2 min

Films with the adequate size for testing their barrier properties were obtained by compression moulding by using a Carver Inc. Hot Press (Wabash, Indiana, USA). In a first step, the different compositions were melted at 170 ºC by keeping them between the plates with no pressure applied for 4 min. Then, pressure was gradually increased up to 5 MPa for 2 min and maintained for 5 extra min, obtaining films with homogeneous thickness (235 ± 15) µm and 14 cm of diameter.

2.3. Characterization methods

161 *2.3.1. Morphological analysis*

162 The microstructure of the fractured surfaces of neat PLA and multifunctional films was
163 investigated by field emission scanning electron microscope (FESEM Supra 25, Zeiss,
164 Germany). Films were previously freeze-cut in liquid nitrogen, gold-coated with an Agar
165 automatic sputter coater and then analysed.

166 *2.3.2. Tensile tests*

167 The tensile tests were performed on rectangular probes as indicated in the EN ISO 527-5
168 standard, with a crosshead speed 1 mm min^{-1}, a load cell 50 N by using a digital Lloyd testing
169 machine (Lloyd Instrument LR 30K Segens worth West, Foreham, UK). Tensile strength (σ_b),
170 failure strain (ε_b), yield strength (σ_y), yield strain (ε_y) and elastic modulus (E) were calculated
171 from the resulting stress-strain curves. The test was performed at room temperature and at least
172 five different samples were tested for each formulation.

173 *2.3.3. Thermal Analysis*

174 Differential scanning calorimetry (DSC) tests were carried out with a TA Instruments Mod.
175 Q200 calorimeter, performing two heating and one cooling scans from -25 °C to 200 °C, at 10 °C
176 min^{-1}. Glass transition (T_g), cold crystallization and melting temperatures (T_{cc} and T_m) and
177 enthalpies (ΔH_{cc} and ΔH_m) for neat PLA and the different formulations were determined during
178 first and second heating scans. The analysis was done in triplicate and the results were reported
179 as the mean value ± standard deviation.

180 Thermal degradation behavior was also evaluated by thermogravimetric analysis (TGA, Seiko
181 Exstar 6300, Tokyo, Japan); 5 mg samples were used and dynamic tests were performed in

nitrogen atmosphere (250 mL min^{-1}) from 30 °C to 600 °C at 10 °C min^{-1}. Thermal degradation temperatures (T_{max}) for each tested material were evaluated.

2.3.4. Barrier Properties

An oxygen permeation analyzer from Systech Instruments (Model 8500) (Metrotec S.A, Spain) was used to performed the Oxygen Transmission Rate (OTR) tests at 23 ± 1 °C. Circular films (14 cm diameter) with an average thickness value between 200 and 250 μm (measured with a Digimatic Micrometer (Series 293 MDC-Lite) (Mitutoyo, Japan) from ten different and random positions), were clamped in the diffusion chamber. An oxygen flux (≥ 99.9 %) was injected at 2.5 bar and the oxygen volumetric flow rate that crossed the film per unit area and time (OTR, cm^3 m^{-2} day^{-1}) was monitored until the steady state was reached. OTR*e (e = thickness, mm) values were calculated for each sample, as the average of three replicates (n =3) ± standard deviation (SD).

Water Vapor Permeability coefficient (WVP) was estimated gravimetrically using the desiccant method described in the ASTM E96/E96 M-05standard (ASTM E-96/E 96M-05). Circular samples (90 mm diameter) were sealed with paraffin to stainless steel dishes containing anhydrous calcium chloride as desiccant agent (pre-dried at 200 °C for 2 h). All dishes were placed in a climate chamber Dycometal-CM81 (Barcelona, Spain) at 23 ± 1 ºC and relative humidity (RH) 50 ± 2 % and they were periodically weighed (24 h intervals) until the steady state was reached. The weight change G, (± 0.001 g) was plotted against elapsed time, t (h) and the slope of the straight line (G/t) is the rate of water vapor transmission, WVT (kg s^{-1} m^{-2}) (Equation (1)).

$$WVT = \frac{G/t}{A} \quad (1)$$

Where A is the test area (0.01 m^2). Then, WVP coefficient is calculated in kg m Pa^{-1} s^{-1} m^{-2} by using Equation (2).

$$WVT = \frac{WVT * e}{\Delta P} \quad (2)$$

Where e (m) is the average film thickness and ΔP is the vapour pressure difference between both sides of the films (Pa), calculated by using Equation (3).

$$\Delta P = S\ (R_1 - R_2) \quad (3)$$

Where S is the vapour pressure of saturation (Pa) at 23 ºC and R_1, R_2 are the relative humidity in the climate chamber and inside the dish, respectively.

Values reported in this work are the average of three replicates tested for each formulation (n = 3) ± standard deviation (SD).

2.3.5. Overall Migration tests

The evaluation of overall migration for all formulations was carried out by using the aqueous food simulant A (ethanol 10 % v/v) in accordance with the Commission Regulation EU (N° 10/2011). Samples were cut (2.5 x 10 cm^2) and immersed in 25 mL of food simulant, keeping in an oven for 10 days at 40 ºC in the case of ethanol 10 % (v/v). After the storage time, samples were removed, and the residual simulants were evaporated in dishes and dried at 105 ºC for 30 min in an oven. The mass of non-volatile residues was determined by using an analytical balance (± 0.1 mg accuracy) until constant weight (± 0.5 mg). The overall migration values were

222 calculated as mg kg^{-1} of simulant, and expressed as the average of three replicates (n =3) ±
223 standard deviation (SD).

224 *2.3.5. Disintegrability under composting conditions*

225 The study of disintegration under composting conditions was carried out by applying the
226 European standard (ISO 20200). Tests were performed at the laboratory-scale to determine the
227 disintegration of plastic materials under simulated intensive aerobic composting conditions at 58
228 ºC and 50% RH. The following formulations were tested: PLA_15PHB_30OLA,
229 PLA_15PHB_30OLA_1CNC, PLA_15PHB_15OLA_10Carv,
230 PLA_15PHB_15OLA_10Carv_1CNC, in order to evaluate the combined effect of CNC, Carv
231 and OLA in PLA_15PHB blends, while neat PLA and PLA_15PHB behaviour under composting
232 conditions were considered as our references.

233 The degree of disintegration D was calculated in percentile by normalizing the sample weight
234 after different days of incubation to the initial weight by using Equation (4):

235 $$D = \frac{m_i - m_r}{m_i} * 100 \quad (4)$$

236 Where, m_i is the initial sample mass, m_r is the dry sample mass after the test.

237 Films with dimensions 15 x 15 x 0.03 mm^3 were weighed and buried into the organic substrate at
238 4-6 cm depth in perforated boxes to guarantee the aerobic conditions. In order to simulate the
239 disintegrability in a real compost, a solid synthetic waste was prepared, mixing sawdust, rabbit
240 food, compost inoculum supplied by Gesenu S.p.a., starch, sugar, oil and urea as indicated in the
241 ISO 20200 standard. Samples were taken out at different times (1, 3, 7, 10, 14 and 17 days),

washed with distilled water and dried in an oven at 37 °C for 24 h. Photographs of samples were taken for visual comparison.

2.3.6. Enzymatic degradation and characterizations

Accelerated enzymatic degradation tests using Proteinase K obtained from Tritirachium album (lyophilized powder, ≥ 30 units/mg protein, Sigma-Aldrich Co) were performed to PLA_15PHB, PLA_15PHB_30OLA and PLA_15PHB_30OLA_1CNC formulations, in order to evaluate, respectively, the effect of plasticizer and the presence of CNC in this polymeric blend loaded with OLA, taking as the control sample PLA_15PHB. Films were cut in sheets (2.2 x 1.3 cm^2) and weighed before their immersion in the degradation medium formed by the enzyme (2 mg) and 5 mL of tris (hydroxymethyl) aminomethane/HCl buffer (0.05 M, pH 8.6) to optimize the enzyme activity. Sodium azide (0.02 wt%) was added to inhibit the microorganisms growth. Enzymatic degradation was performed at 37 ºC in an incubator and the buffer-enzyme system was renewed every 24 h for 7 days to maintain the enzymatic activity. Specimens (in triplicate) of each formulation were removed from the solution every 24 h, washed with distilled water and dried at room temperature up to constant weight, determined using an analytical balance (± 0.0001 g). The weight loss of each sample at different incubation times (t) was calculated by using Equation (5):

$$\text{Weight loss} = [(W_0 - W_t) / W_0] \times 100\% \quad (5)$$

Where W_0 represents the initial weight of a specimen and W_t is the dry weight of the same specimen after different incubation times. All values reported were the average of measurements for three replicate specimens (± SD).

Visual observations were performed for each specimen, while thermal characterization by DSC analysis and morphological evaluation by scanning electron microscopy (SEM) were also carried out after different incubation times. DSC tests were performed by following the same conditions already indicated in the characterization section, and using a TA Instruments DSC Q2000 (New Castle, DE, USA). Glass transition, cold and melting crystallization temperatures and enthalpies were evaluated in all formulations after 0, 1, 3, 5 and 7 days of incubation during the first heating scan. Surface and cross-section morphologies of the specimens at 0, 3 and 7 days were evaluated by using a JEOL model JSM-840 (Jeol USA Inc., Peabody, USA) scanning electron microscope, operated at 10 kV. Samples were sputtered with gold prior to analysis.

2.4. Statistical analysis

One-way analysis of variance (ANOVA) was performed on data obtained from barrier and migration analyses. The statistical program Statgraphics Centurion 16.1.18 was used and the Tukey's multiple sample comparison test with 95 % confidence level ($p < 0.05$) was applied to identify significance differences between data.

3. Results and Discussion

3.1. Microstructure

The evaluation of the filler dispersion and the interface among different phases in plasticized PLA_15PHB blends containing carvacrol was performed. **Figure 1**, **panel A** shows FESEM images of PLA, PLA_15PHB and PLA_15PHB plasticized with OLA (30 wt%). Furthermore multifunctional systems combined with OLA (15 wt%) and Carv (10 wt%) with and without 1 wt%, of CNC, were detailed evaluated by FESEM at different resolutions (**Fig. 1, Panel B**).

Neat PLA showed a smooth and uniform fractured surface (Armentano, et al., 2015b), while FESEM images of PLA_15PHB films showed a rough fractured surface and phase separation with dispersed PHB phase and relatively small average diameter (**Fig. 1 Panel A, b**), as already reported (Arrieta, Fortunati, Dominici, Lopez, & Kenny, 2015).

In those formulations plasticized with OLA (**Fig. 1 Panel A, c**) the plastic deformation induced by the presence of the plasticizer on the fractured surfaces was observed. Similar results were reported in the case of formulations of PLA_PHB plasticized with acetyl(tributyl citrate) (ATBC) (Arrieta, Fortunati, Dominici, Lopez, & Kenny, 2015). The effect of the plastic deformation was still visible in the system with CNC (PLA_15PHB_30OLA_1CNC, **Figure 1 Panel A, d)**. In films containing carvacrol (PLA_15PHB_15OLA_10Carv), nano-separated phases were observed (Burgos, et al., 2017) (**Fig. 1 Panel A, e**) insert). This effect was more evident in PLA_15PHB_15OLA_10Carv_1CNC (**Fig. 1 Panel A, f**). Moreover, two different regions were clearly visible in the fracture surface of PLA_15PHB_15OLA_10Carv formulation with ductile and brittle morphologies. Finally, the addition of CNC (PLA_15PHB_15OLA_10Carv_1CNC, **Fig. 1 Panel A, f) and Fig. 1 Panel B (a-d)** at different magnifications) resulted in phase separation, uniformly distributed along the fractured surface section. No evidence of aggregation of CNC is visible in the fracture surface, underlining a good dispersion of a bio-based nanofillers.

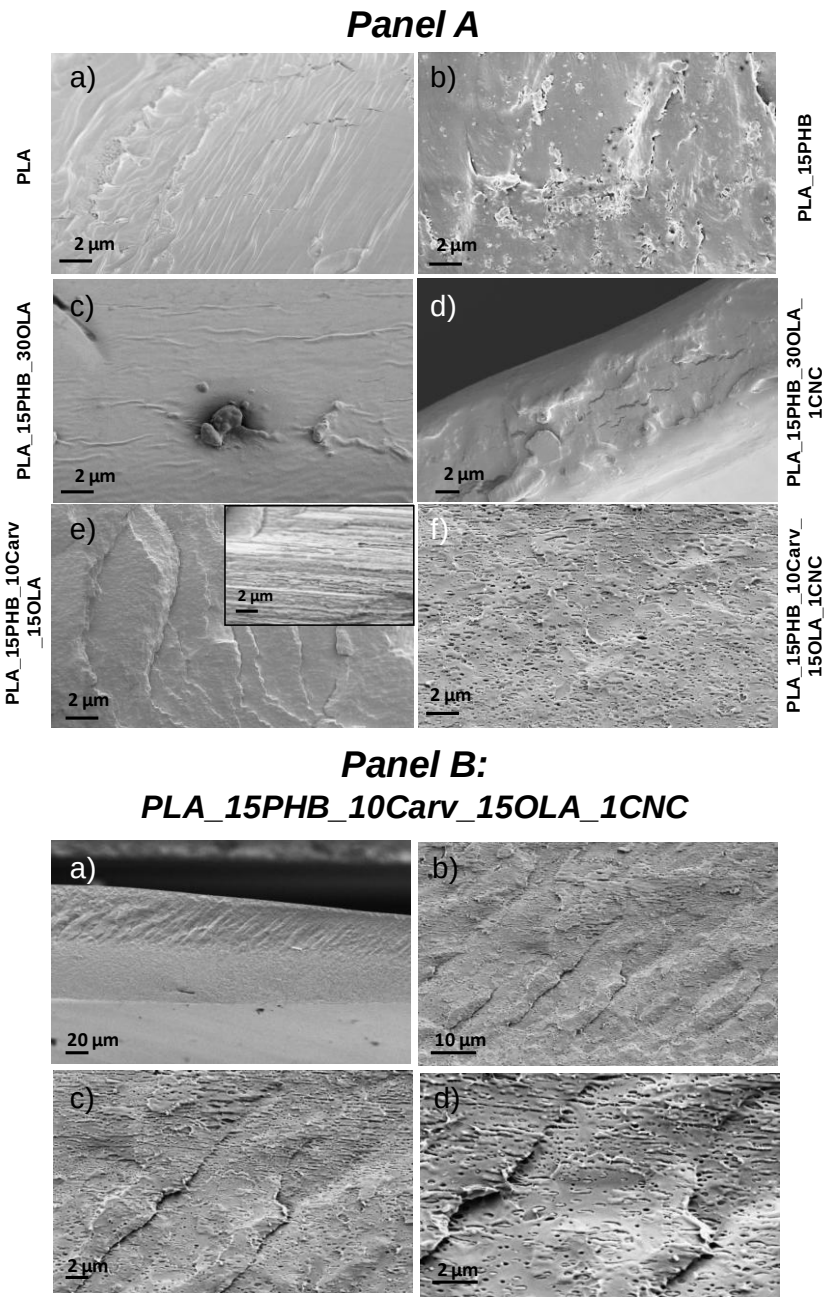

302

303 **Figure 1.** Panel A: FESEM images of cryo-fractured surfaces of PLA (a), PLA_PHB (b), PLA_PHB_30OLA (c),
304 PLA_PHB_30OLA_1CNC (d), PLA_PHB_10Carv_15OLA (e) and PLA_PHB_10Carv_15OLA_1CNC (f); Panel
305 B: FESEM images of cryo-fractured surfaces at different magnifications of PLA_PHB_10Carv_15OLA_1CNC film
306 (a-d).

307 The presence of CNC combined with OLA and carvacrol during processing induced the
308 formation of elliptical shape/lengthened regions, oriented in the machine direction (extrusion-

filmature) (Fig. 1 Panel B). This phenomenon could be correlated to the interaction of the CNC with the other components. In fact, the combination of PLA, PHB, OLA and Carv (PLA_PHB_10Carv_15OLA) did not highlight the presence of a phase separation (Fig. 1, Panel A, e). This positive phenomenon was due to the affinity among the different components, that could be estimated by the solubility parameter (δ) of four components used to develop PLA based film (PLA_PHB_10Carv_15OLA). Since the difference in the Hildebrand solubility parameters (δ) are relatively low: PLA (δ=19.1-20 $MPa^{1/2}$,), PHB, (δ=18.5-20.1 $MPa^{1/2}$), OLA (δ=17.7 $MPa^{1/2}$), and carvacrol (δ=15.1 $MPa^{1/2}$) (Arrieta, Samper, Aldas, & Lopez, 2017), good miscibility between different components should be expected.

3.2. Mechanical analysis

The evaluation of the mechanical performance in polymer matrices is one of the most important properties to be evaluated. In general terms, most polymer-based formulations intended for packaging require flexibility to avoid breakage during use and a hardness value suitable for reducing the risk of perforations during their life cycle. Mechanical performance of PLA and PLA_15PHB based formulations was evaluated by tensile tests and the results are summarized in **Figure 2 Panel A**, while the stress-strain curves are reported in **Panel B**. Neat PLA showed 100% elongation at break and a value of the elastic modulus of 1300 MPa. The incorporation of PHB to PLA-based films did not significantly modify the elastic modulus and only a slight increase in the elongation at break to 100% was observed (Armentano, et al., 2015; Armentano, et al., 2015b). The stress-strain curves of PLA and PLA_15PHB showed a similar shape (**Fig. 2, Panel B**). The effect of the different content of CNC was evaluated in PLA_15PHB formulations. Although no increase in the Young's modulus values was detected for the PLA_15PHB_1CNC and PLA_15PHB_3CNC formulations (**Fig. 2, Panel A**), a slight increase

in the elongation at break value for the PLA_15PHB_1CNC film with respect to both, the PLA matrix and the PLA_15PHB blend film was registered. This behavior can be related to an efficient dispersion of CNC and at the nanometer level, obtained during the extrusion process at the selected conditions. The good dispersion of CNC in polymeric based systems determines an enhancement in the interfacial adhesion and consequently a better interaction between PLA and PHB induced by the cellulosic nanofillers (Fortunati, et al., 2014). However, when CNC were added at 3 wt% to PLA_15PHB formulations, no particular enhancement in the mechanical behavior was obtained when compared to PLA and PLA_15PHB reference systems (**Fig. 2**). On the basis of these results, 1 wt% of CNC was selected as the more suitable content in the production of four- and five-components based films with OLA and/or Carvacrol. In fact, the positive effect of 1 wt% of CNC was also evaluated and confirmed in the PLA_15PHB_30OLA and PLA_15PHB_15OLA_10Carv systems. In the case of the PLA_15PHB_30OLA_1CNC films, a simultaneous increase in the elongation at break (PLA_15PHB_30OLA_1CNC = 430% while PLA_15PHB_30OLA = 370%) and the Young's modulus (about 730 MPa for the four-component system and 590 MPa for the PLA_15PHB_30OLA reference film). A similar behavior was also detected for the PLA_15PHB_30OLA_10Carv_1CNC five-component films, showing 410 % of elongation at break while it was 150 % for the PLA_15PHB_30OLA_10Carv reference film, while reaching elastic modulus 710 MPa while it was 330 MPa for the PLA_15PHB_30OLA_10Carv reference formulation (Fortunati, et al., 2014; Nostro & Papalia, 2012; Shi, et al., 2012). Therefore, the reinforcement effect of CNC when OLA and carvacrol are used as plasticizer and antibacterial additives respectively, can be attributed to the homogenous dispersion of CNC in the selected bio-based additives.

These results underlined the positive effect of the addition of CNC to PLA-based matrices and their interaction with OLA and carvacrol in PLA_15PHB blends, both in the elastic and plastic region, suggesting the prospective applicability of these films as multifunctional systems with a broad range of mechanical properties. The mechanical property results permits to evaluate the role of the plasticizer, that mainly increases the elongation at break, but without decreasing too much the Young modulus; while the introduction of CNC permit to increase the Young modulus, that shows a decreasing in the sample with the high content of OLA and Carvacrol. The good nanodispersion of the CNC is also demonstrated by the high level of elongation factor, that increase until 400%.

Moreover, good dispersion and a good CNC-matrix interaction contributes to dissipate energy from external stresses, which enhances the mechanical properties of the nanocomposites.

Panel A

Formulations	σ_Y (MPa)	ε_Y(%)	σ_b(MPa)	ε_b (%)	E_{YOUNG} (MPa)
PLA	37±5	3.4±0.4	35±6	100±30	1300±180
PLA_15PHB	40±5	3.8±0.5	31±5	140±60	1220±140
PLA_15PHB_CNC films					
PLA_15PHB_1CNC	34±4	3.1±0.1	30±5	210±40	1300±200
PLA_15PHB_3CNC	36±5	3.2±0.4	29±2	80±50	1280±100
PLA_15PHB_30OLA films					
PLA_15PHB_30OLA	16±3	3.9±0.4	19±3	370±20	590±50
PLA_15PHB_30OLA_1CNC	20±2	3.5±0.1	16 ±2	430±40	730±80
PLA_15PHB_15OLA_10Carv films					
PLA_15PHB_15OLA_10Carv	16±2	20±2	15±2	150±30	330±60
PLA_15PHB_15OLA_10Carv_1CNC	16±2	4.0±0.1	16±2	410±50	710±60

Panel B

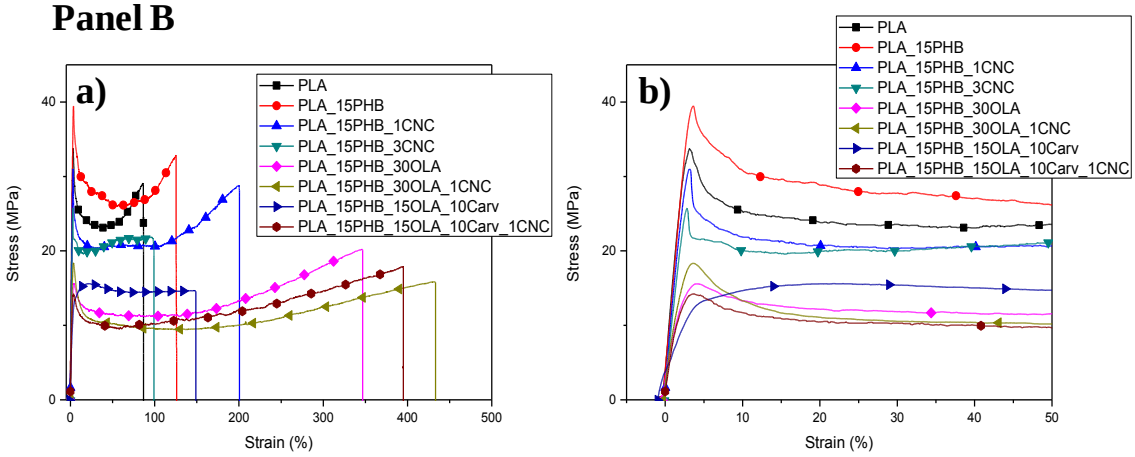

Figure 2: Panel A: Mechanical Properties of PLA and PLA_15PHB films. Panel B: Stress-strain curves of PLA based formulations (a, b (zoom))

3.3. Thermal Properties

The thermal properties of PLA and PLA_15PHB-based formulations were investigated by using differential scanning calorimeter (DSC) and thermogravimetric analysis (TGA). The effect of CNC and their combination with the other components of these blends (PHB, OLA and Carvacrol) on the thermal properties of PLA matrix was evaluated. DSC thermal parameters obtained during the first and the second heating scan have been summarized in **Tables 2**.

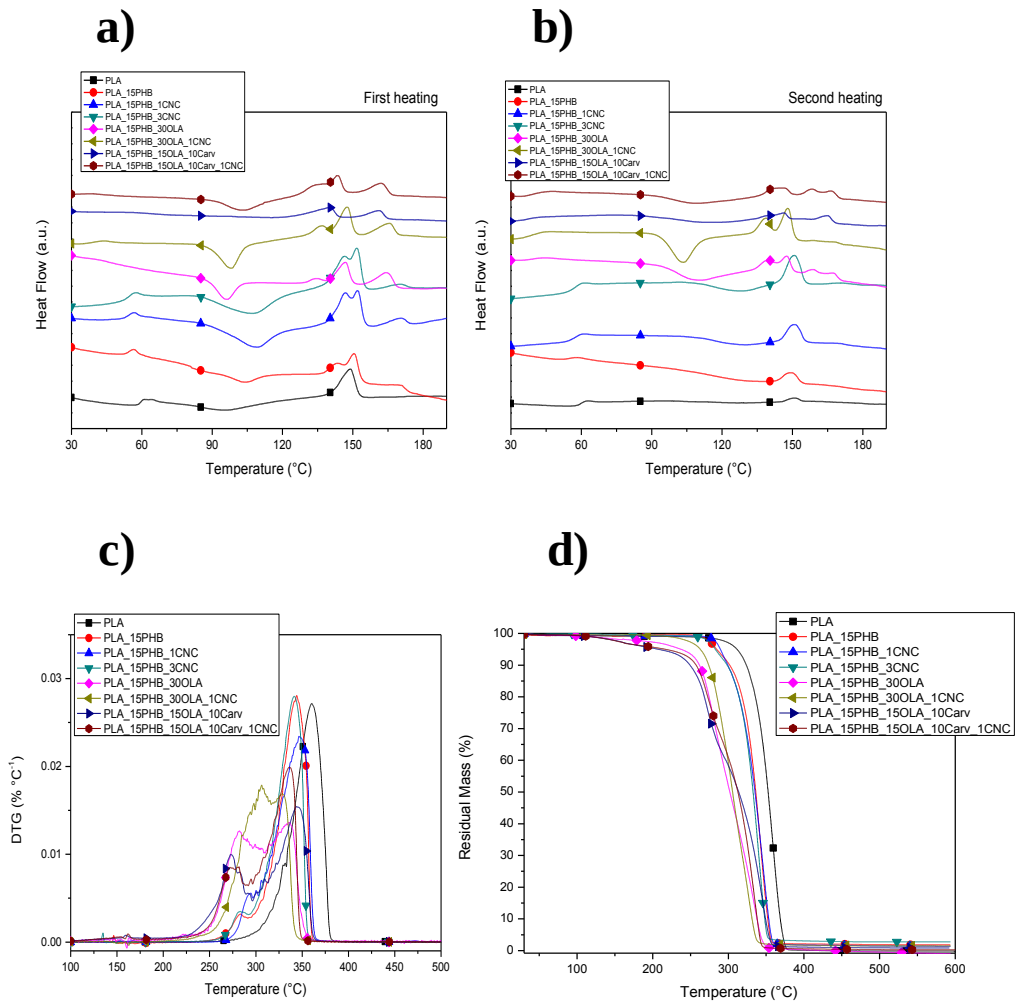

375

376 **Figure 3.** DSC thermograms at first (a) and second (b) heating scan; TGA derivative (DTG) (c) and residual mass
377 curves (d) of PLA based formulations.

378 The thermograms for the first and second heating scans are reported in **Figure 3 a** and **b**,
379 respectively. As previously reported in literature, PLA neat films during the first heating scan
380 showed a glass transition temperature (T_g) around 60 °C (Armentano et al., 2015b), the cold
381 crystallization exotherm with its maximum (T_{cc}) around 95 °C and the melting endotherm peak
382 obtained close to 150°C; a similar behavior was also observed for the second heating scan.
383 Furthermore, a slight shift to lower T_g values at first (**Fig. 3 a and Table 2**) and second heating
384 scans (**Fig. 3b, Table 2**) was detected for the PLA_15PHB blend, that also showed a multi-step

melting process (Armentano et al., 2015b), (**Fig. 3a, b**). It can be concluded that the first and second melting temperatures (T'_m and T''_m) were due to the formation of different crystal structures during heating, as reported also for other polymeric blends (Armentano et al., 2015a; Martino et al., 2011), while the third melting temperature (T'''_m) corresponds to the melting of PHB around 170 °C, (Armentano et al., 2015a,; Burgos al., 2017), underlining the partial miscibility between PLA and PHB. The introduction of CNC at 1 wt% in PLA_15PHB blends did not result in noticeable modifications in the T_g values, while an evident increase in the cold crystallization enthalpy and a consequent increase in the melting enthalpy respect to the blend was revealed during the first heating scan, underling the nucleation effect of cellulose even at this low content (**Table 2**). A similar effect was also observed during the second heating scan (**Table 2**). On the contrary, no particular differences were detected when a higher content of CNC (3 wt%) was added to the PLA_15PHB blend during the first heating scan (**Table 2**), whereas the presence of CNC produced an increase in the cold crystallization enthalpy and a consequent slight increase in the melting enthalpy value during the second heating scan (**Table 2**). The presence of OLA and Carv shifted the melting temperature of PLA and PHB components to lower temperatures at first and second heating scan as expected by their plasticization effect to the polymer matrix. The addition of 1 wt% CNC to the PLA_15PHB_30OLA formulation produced a slight increase in both, the glass transition and the melting enthalpy, during the first heating, confirming the role of CNC as nucleation agents even in plasticized PLA-based formulations. Finally, this effect was more evident in the PLA_15PHB_15OLA_10Carv_1CNC systems, where the presence of CNC induced a slight increase in the glass transition temperature at the first and second heating scans (**Table 2**).

Table 2. Thermal properties of PLA and PLA_15PHB films: from DSC analysis (First and second heating scan) and thermal degradation temperature (T_{max}) measured from DTG curves during the TGA test.

	DSC, First Heating Scan							***TGA***
Formulations	**T_g (°C)**	**T_{cc} (°C)**	**ΔH_{cc}(J/g)**	**T'_m (°C)**	**T''_m (°C)**	**T'''_m(°C)**	**ΔH_m(J/g)**	**T_{max}(°C)**
PLA	60.1±1.0	95.1±0.8	15.8±0.7	150.0±0.5	-	-	27.6±0.4	361±1
PLA_15PHB	55.4±1.2	103.6±0.5	9.3±0.6	144.0±0.9	150.2±0.5	170.4±1.0	25.4±0.5	349±1
PLA_15PHB_CNC films								
PLA_15PHB_1CNC	52.4±2.3	109.3±1.0	32.8±1.1	147.4±0.6	152.5±0.2	170.5±0.9	39.7±0.5	347±2
PLA_15PHB_3CNC	53.4±0.5	107.0±0.2	32.1±0.2	147.2±0.1	152.0±0.1	170.0±0.2	41.2±1.4	341±1
PLA_15PHB_30OLA films								
PLA_15PHB_30OLA	36.2±1.4	95.6±0.5	22.6±0.7	134.6±0.5	146.1±0.6	164.8±0.5	34.1±0.2	336±1
PLA_15PHB_30OLA_1CNC	40.8±0.4	97.8±0.6	24.8±0.6	137.8±0.4	148.2±0.4	165.0±1.0	44.4±0.6	327±2
PLA_15PHB_15OLA_10Carv films								
PLA_15PHB_15OLA_10Carv	35.9±1.6	-	-	139.9±0.5	-	160.6±0.5	34.3±0.8	345±1
PLA_15PHB_15OLA_10Carv_1CNC	37.1±2.6	102.6±0.6	23.8±1.2	135.1±1.3	143.8±0.5	161.9±0.7	32.9±1.5	336±1
	DSC, Second Heating Scan							
Formulations	**T_g (°C)**	**T_{cc} (°C)**	**ΔH_{cc}(J/g)**	**T'_m (°C)**	**T''_m (°C)**	**T'''_m (°C)**	**ΔH_m(J/g)**	
PLA	59.3±0.3	126.2±0.5	2.5±0.2	151.2±0.4	-	-	3.1±0.1	
PLA_15PHB	54.7±0.2	127.8±0.4	2.5±0.4	148.9±0.7	-	170.1±0.5	6.3±0.7	
PLA_15PHB_CNC films								
PLA_15PHB_1CNC	56.3±0.7	129.1±0.3	6.8±0.4	150.9±0.2	-	169.4±0.2	12.7±0.5	
PLA_15PHB_3CNC	57.1±0.2	129.1±0.9	12.01±0.6	151.3±0.1	-	170.6±06	15.7±0.8	
PLA_15PHB_30OLA films								
PLA_15PHB_30OLA	38.6±0.1	108.2±0.6	21.5±0.3	139.7±0.4	147.5±0.6	159.1±0.1/ 167.4±0.2	37.9±0.5	
PLA_15PHB_30OLA_1CNC	40.2±0.1	105.1±0.6	28.5±0.5	139.1±0.8	142.8±0.4	167.0±0.7	34.8±0.6	
PLA_15PHB_15OLA_10Carv films								
PLA_15PHB_15OLA_10Carv	36.7±1.8	115.9±1.2	7.2±0.2	137.1±1.4	145.7±0.4	153.8±0.1/ 163.1±1.3	34.3±0.8	
PLA_15PHB_15OLA_10Carv_1CNC	41.5±1.8	107.9±1.2	12.2±1.9	141.0±0.5	146.2±0.3	158.2±0.5/ 167.0±0.2	32.0±3.0	

410 This phenomenon was due to the presence of CNC that tend to reduce the chain mobility
411 (Fortunati et al., 2014; Arrieta, Fortunati, Dominici, & Lopez, Kenny, 2015), in agreement with
412 the results of tensile tests previously discussed, that underline the increase in the elastic modulus
413 in the five-components formulations when compared to the four-component system
414 (PLA_15PHB_15OLA_10Carv) (**Fig. 2**). Furthermore, the presence of the T_{cc} signal, not evident
415 for the PLA_15PHB_15OLA_10Carv film in the first heating, confirmed the potentiality of CNC
416 as nucleation agents even when two compounds with plasticizing effect (OLA and Carvacrol),
417 were added to the PLA_15PHB blend. Thermogravimetric analysis was performed in order to
418 establish the effect of CNC and their combination with the other components (PHB, OLA and
419 Carvacrol) on the thermal properties of the PLA matrix. Temperatures for the maximum
420 degradation rate for different formulations are summarized in **Table 2**, while derivative curves
421 (DTG) and residual mass curves are shown in **Fig. 2c and 2d,** respectively.

422 It was observed that the neat PLA film degraded in a single step process with a maximum
423 degradation peak (T_{max}) at 361 °C, while a two-steps degradation behavior was observed in the
424 case of the PLA_15PHB blend (the first peak at temperatures around 280 °C corresponding to
425 the PHB thermal degradation, while a second degradation peak, attributed to the PLA
426 degradation, shifted to lower temperatures (T_{max} 349 °C) (Armentano et al., 2015b). The
427 presence of CNC at 1 wt% in the PLA_15PHB blend did not alter the maximum degradation
428 temperature, while producing a shift to higher temperatures of about 13 °C in the first
429 degradation step (293 °C for the PLA_15PHB_1CNC with respect to 280 °C for the
430 PLA_15PHB blend), underlining the positive effect of CNC added at 1 wt% on preventing
431 thermal decomposition of the PLA matrix during the melt compounding. CNC improves the
432 thermal stability of PHB. The presence of OLA induced a decreased in the onset degradation

temperature in the PLA_PHB polymeric blend, with an evident decrease (around 13 °C) in the temperature for the main degradation peak, but the presence of 1 wt% of CNC in the PLA_15PHB_30OLA formulation produced a shift to higher temperatures of around 20 °C for the first degradation step and a decrease of about 9 °C of T_{max}. A similar effect was detected for the first degradation step of the PLA_15PHB_30OLA_1CNC system. On the contrary, the addition of 3 wt% of CNC to the ternary formulation produced a decrease of about 8 °C in T_{max} when compared to the PLA_15PHB blend and no particular effect on the first degradation step was induced by this higher amount of cellulose. Moreover, it should be noted that the introduction of 1 wt% of CNC in four- and five-component based formulations resulted in shift to lower values (of about 9 °C) of the maximum degradation temperatures, although processing windows were broad enough to avoid any risk of thermal degradation during processing, since no degradation was observed in the temperature region from room temperature to 200 °C, where the bionanocomposites were processed and/or are intended to be used.

3.4. Barrier Properties

The barrier properties of PLA and PLA_15PHB formulations were studied by the determination of the oxygen transmission rate (OTR) and water vapor permeability (WVP) of films, in order to estimate the effect of the addition of CNC and their combination with PHB, OLA and carvacrol on the barrier properties of PLA films. The obtained data are summarized in **Table 3**. The addition of 1 wt% of CNC to PLA_15PHB did not induce significant ($p< 0.05$) changes in the OTR*e and WVP values, maintaining the improvement in the oxygen and water vapor barrier properties of PLA gained as a consequence of the high crystallinity of PHB (Arrieta, Fortunati, Dominici, Lopez, & Kenny, 2015). The incorporation of CNC at 3 wt% to the PLA_15PHB formulation increased significantly ($p< 0.05$) the OTR*e mean value up to ca. 129 %, while no

significant effect was observed in WVP values. This result confirmed the selection of 1 wt% of CNC in the production of formulations with OLA and/or carvacrol, as already discussed in previous sections.

Table 3. Oxygen Transmission Rate per film thickness (OTR·e) and Water Vapor Permeability (WVP) coefficients of PLA and PLA_15PHB films.

Formulations	OTR*e (cm^3 mm m^{-2} day^{-1})	WVP x 10^{14} (kg m Pa^{-1} s^{-1} m^{-2})
PLA	22.9 ± 0.4^{ad}	1.88 ± 0.21^{ad}
PLA_15PHB	14.9 ± 0.8^{ab}	1.54 ± 0.20^{b}
PLA_15PHB_CNC films		
PLA_15PHB_1CNC	13.3 ±1.4^{b}	1.59 ± 0.28^{ab}
PLA_15PHB_3CNC	34.1 ± 12.4^{c}	1.31 ± 0.19^{b}
PLA_15PHB_30OLA films		
PLA_15PHB_30OLA	18.6 ±1.4^{abd}	0.97 ± 0.13^{c}
PLA_15PHB_30OLA_1CNC	24.7 ± 6.4^{d}	1.28 ± 0.22^{bc}
PLA_15PHB_15OLA_10Carv films		
PLA_15PHB_15OLA_10Carv	63.3 ± 2.8^{e}	2.03 ± 0.11^{d}
PLA_15PHB_15OLA_10Carv_1CNC	25.6 ± 4.6^{cd}	1.41 ± 0.18^{b}

$^{a\text{-}e}$ *Different superscripts within the same column indicate significant differences between formulations ($p < 0.05$)*

$n = 3$, mean ± SD.

It was observed that the addition of OLA plasticizer reduced barrier properties of PLA_PHB polymeric blend films, due to the increase in free volume, that favors the diffusion of water molecules through the films.

In the plasticized PLA_PHB films (plasticizer content: OLA=30wt%), the presence of CNC did not significantly modify the barrier properties of the PLA_15PHB_30OLA films. This result denoted that the effect of CNC on the chain mobility observed in the thermal and mechanical

analysis was not strong enough against the increase in permeability that the presence of OLA at 30 wt% induced in the PLA_15PHB blend, such as the development of PLA crystallinity and the increase of chain mobility (Armentano et al., 2015b).

However, in the PLA_15PHB_15OLA_10Carv_1CNC system significant decreases ($p < 0.05$) in OTR*e and WVP values were observed (around 60 % and 31 %, respectively) (**Table 3**), comparing to those values obtained for the plasticized blend before the addition of CNC. It should be noted that the incorporation of OLA and carvacrol to the PLA_PHB blend produced a significant deterioration of the oxygen and water vapor barrier properties, which has been mainly related with the strong plasticizing effect of OLA and the decrease in the hydrophobic character of the PLA_15PHB blend caused by the presence of both additives (Burgos et al., 2017). The significant improvement of the oxygen and water vapor barrier properties in this five-components formulation with respect to the PLA_15PHB_15OLA_10Carv film could be associated to the nucleation effect of CNC that tend to decrease the mobility of the macromolecular chains, in agreement with the DSC and tensile tests results previously discussed.

The presence of CNC in the plasticized blend leads a more tortuous path to permeation of water and oxygen molecules, improving the barrier properties. Moreover, the decrease in the hydrophobic character of the blend provided by the high amount of hydroxyl groups of CNC, OLA and carvacrol (Nostro & Papalia, 2012; Dhar, Bhardwaj, Kumar, & Katiyar, 2015) favored hydrogen bond interactions with the carbonyl groups of PLA and PHB, resulting in an overall improvement of the barrier properties (Arrieta, Samper, Aldas, & Lopez, 2017; Arrieta, Fortunati, Dominici, Lopez & Kenny, 2015). In this sense, the OTR*e and WVP values obtained from the five-components formulation did not differ significantly from those observed for the PLA_15PHB formulation, but the multifunctional films show high values of elongation at break

and antibacterial character (Burgos al., 2017). Other authors reported similar effects on the oxygen and water vapor barrier properties of PLA (Dhar, Bhardwaj, Kumar, & Katiyar, 2015; Sanchez-Garcia, & Lagaron, 2010) and PLA_PHB blends (Arrieta et al., 2014b) after the incorporation of cellulose-based nanostructures.

3.5. Migration properties

Overall migration tests in aqueous simulant were performed to evaluate the total amount of non-volatile substances that could pass from the plastic material to aqueous food, which must be lower than the overall migration limit required by the current normative (60 mg kg^{-1}) for food packaging materials. In this study, the effect of the incorporation of 1 wt% of CNC into the overall migration values of the plasticized and unplasticized PLA_15PHB formulations were evaluated in ethanol 10 % (v/v) (**Table 4**). It was observed that the overall migration values obtained from ethanol 10 % (v/v) tests were below the legislative limit of 60 mg kg^{-1} in all samples, with no detection of non-volatile compounds in the PLA_15PHB_15OLA_10Carv sample. This result could be explained by the presence of OLA and carvacrol in the PLA_15PHB blend, which improve the hydrophobic character of the polymer blend and increase the interactions between hydroxyl groups of carvacrol and OLA with both polymers (Armentano et al, 2015b). It should be noted that the incorporation of 1 wt% of CNC to PLA_15PHB and PLA_15PHB_30OLA blends decrease significantly ($p < 0.05$) their overall migration rates, reaching values lower than 13 mg kg^{-1} with no significant differences between them.

Table 4. Overall migration values (mg kg^{-1}) in ethanol 10 %(v/v) for PLA and PLA_15PHB films.

Formulations	**Ethanol 10 (v/v) % (mg kg^{-1})**
PLA	19 ± 2^{ac}
PLA_15PHB	27 ± 9^{a}
PLA_15PHB_CNC films	
PLA_15PHB_1CNC	8 ± 4^{b}
PLA_15PHB_30OLA films	
PLA_15PHB_30OLA	27 ± 6^{a}
PLA_15PHB_30OLA_1CNC	12 ± 4^{bc}
PLA_15PHB_15OLA_10Carv films	
PLA_15PHB_15OLA_10Carv	n.d.
PLA_15PHB_15OLA_10Carv_1CNC	11 ± 2^{bc}

$^{a-c}$ Different superscripts within the same column indicate significant differences between formulations ($p < 0.05$)

n.d.: not detected, n = 3, mean ± SD.

(Luzi et al., 2015) This behavior could be related to the efficient dispersion of the nanocrystals, resulting in better interactions of CNC with the polymer matrix, OLA and carvacrol, as previously reported (Fortunati et al., 2014). The migration results underlined the positive effect of the incorporation of 1 wt% CNC, that could act nucleating agents increasing the interactions with OLA and carvacrol, as previously underlined and discussed with the FESEM micrographs (**Fig. 1 Panel A f**) and **Fig. 1 Panel B (a-d))** in the polymer matrix and consequently restricting their release into the food simulant. In addition, the presence of CNC in the five-components film induced the absorption of additives limiting the migration of different components.

3.6. Disintegrability under compositing conditions and enzymatic degradation studies

The post-use performance of all PLA-based formulations was analysed by performing disintegrability tests under composting conditions, according to the ISO 20200 standard, (ISO20200) whereas the enzymatic degradation study by using Proteinase K was conducted on PLA_15PHB, PLA_15PHB_30 OLA and PLA_15PHB_30 OLA_1CNC films. **Figure 4a** shows images of all different PLA-based formulations at the beginning of the test and after several incubation times, while **Figure 4b** reports disintegration values for the same materials. It was observed that all samples changed their color and dimensions just after the first days of incubation, as a consequence of the hydrolitic process and because of the low thicknesses of films used for this test. In particular all formulations became white and opaque after 3 days, while the first fractures appeared visibly distinguishable after only 7 days, as previously reported for similar systems (Arrieta, Fortunati, Dominici, Lopez, & Kenny, 2015).

The presence of the different components (PHB, OLA, Carvacrol and CNC) modified the degradation kinetic and the weight loss values respect to PLA film. This effect was particularly evident for the PLA_15PHB film, that showed the lowest value of disintegration (around 50%) at 14 days, due to the higher crystallinity induced by the PHB polymer (Arrieta, Lopez, Rayon, &Jimenez, 2014d), while the presence of plasticizers (OLA and carvacrol), especially when combined, facilitated the disintegration of PLA_15PHB_15OLA_10Carv and PLA_15PHB_15OLA_10 Carv_1CNC formulations (60-70 % of disintegration at 14 days). The presence of CNC did not significantly modify the disintegration processes, while all the formulations disintegrated (reaching disintegrability values close to 90%) after 17 days of test (**Fig. 4 a,b**). All material tested are visible disintegrated after 17 days, according to the ISO20200. Disintegrability in composting conditions is an important evaluation in order to test the end use of the bio-based multifunctional nanocomposites based on PLA.

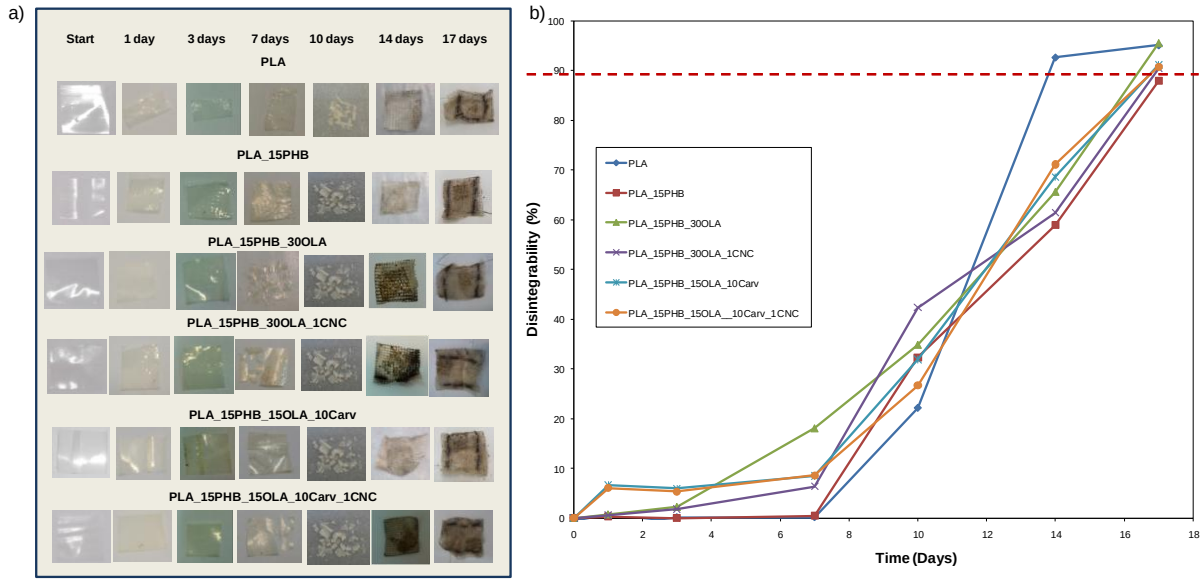

549

550 **Figure 4.** Visual observation (a) and disintegrability values (b) of PLA, PLA PLA_15PHB, PLA_15PHB_30OLA,
551 PLA_15PHB_30OLA_1CNC, PLA_15PHB_15OLA__10Carv and PLA_15PHB_15OLA__10Carv_1CNC before
552 and after different days in composting conditions.

553 The enzymatic degradation of the PLA_15PHB_30OLA and PLA_15PHB_30OLA_1CNC
554 formulations was performed in the presence of Proteinase K in order to evaluate the effect of
555 OLA and CNC on the enzymatic degradation of PLA_15PHB blends, used as control samples. It
556 has been reported that this enzyme should be absorbed by the polylactide substrates in order to
557 catalyze their hydrolytic degradation. The scission of the polymer chains preferentially occurs in
558 the amorphous regions, getting progressively smaller segments (low molecular weight oligomers,
559 dimers and monomers) that finally degrade into carbon dioxide and water (Zhao, et al., 2008;
560 Wang, Fan & Hsiue, 2005). The main factors affecting the enzymatic degradation rate of PLA
561 are molecular weight, hydrophilicity, degree of crystallinity, morphology, presence of additives
562 and polymer blending (Tsuji, Echizen, & Nishimura, 2006). **Figure 5a** shows the images
563 obtained from the macroscopic observation of the PLA_PHB based formulations at different
564 incubation times. Just after 24 h of incubation all samples turned from transparent to translucent
565 or even opaque (Luzi, et al., 2015). The increase of opacity at short incubation times could be

566 related to changes in the material structure due to the hydrolytic process and/or increase in
567 crystallinity caused by the accommodation of chain fragments during degradation (Arrieta,
568 Samper, Aldas, & Lopez, 2017). Moreover, all samples progressively lost their structural
569 integrity with incubation time in a similar way, resulting in a significant reduction in their
570 thickness and showing visible phenomena of cracking and fragmentation, especially from the
571 fourth day of testing onwards. **Figure 5 b** shows the evolution of weight loss of PLA_15PHB,
572 PLA_15PHB_30OLA and PLA_15PHB_30OLA _1CNC films with time during enzymatic
573 incubation with Proteinase K. As it was expected, all films showed a linear increase in weight
574 loss with incubation time up to the fourth day, without any induction period, as previously
575 reported for PLA systems under similar experimental conditions (Arrieta, Samper, Aldas, &
576 Lopez, 2017; Tsuji & Miyauchi, 2001). The incorporation of 1 wt% CNC to the plasticized
577 PLA_15PHB blends did not produce significant differences in their weight loss data and
578 degradation rates during the entire test (**Fig. 5 b**). However, data obtained for the
579 PLA_15PHB_30OLA and PLA_15PHB_30OLA _1CNC formulations were clearly higher than
580 those obtained for the PLA_15PHB blend, up to the fourth day of incubation, with a greater
581 extent for the sample with CNC.

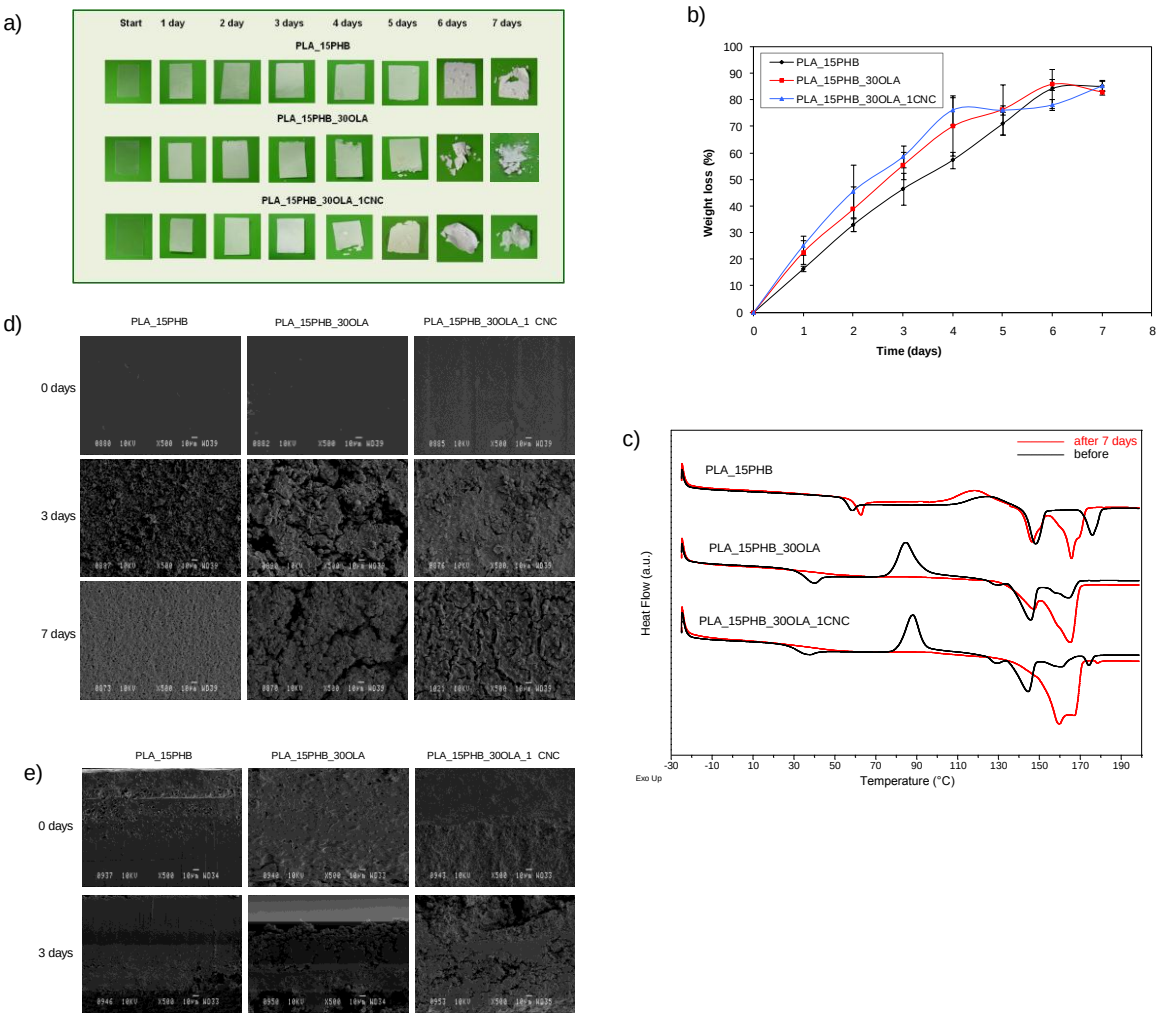

582

583

584 **Figure 5.** Images of the individual samples (PLA_15PHB, PLA_PHB_30OLA and PLA_PHB_30OLA_1CNC)
585 before and after different incubation times at 37 ºC during enzymatic degradation with Proteinase K (a); weight loss
586 of PLA_15PHB, PLA_PHB_30OLA and PLA_PHB_30OLA_1CNC films as a function of incubation time during
587 enzymatic degradation with Proteinase K at 37 ºC (b); DSC curves of PLA_15PHB, PLA_15PHB_30OLA and
588 PLA_15PHB_30OLA_1CNC films during the first heating scan, before and after 7 days of enzymatic degradation at
589 37 ºC with Proteinase K (c); SEM micrographs of surfaces (x500) of PLA_15PHB, PLA_PHB_30OLA and
590 PLA_PHB_30OLA_1CNC films at 0, 3 and 7 days of enzymatic degradation test (d) and SEM micrographs of
591 cross-sections (x500) of PLA_15PHB, PLA_15PHB_30OLA and PLA_15PHB_30OLA_1CNC films before and
592 after 3 days of enzymatic degradation test (e).

593

594 The presence of CNC and the higher amount of low molar mass chains provided by OLA could

595 act as enzymatic attack points during the first days of degradation. At the end of the total

incubation period, all formulations achieved similar average weight loss values (80-85 %). On the other hand, control samples placed in the buffer solution without the presence of the enzyme and incubated under similar conditions did not show significant weight loss (< 1.5 %) at

Table 5. DSC thermal parameters (first heating scan at 10 ºC min^{-1}) obtained for samples at 0, 1, 3, 5 and 7 days of enzymatic degradation.

Formulations	Days	T_g (ºC)	T_{cc} (ºC)	ΔH_{cc} (J g^{-1})	T_m' (ºC)	T_m'' (ºC)	T_m''' (ºC)	ΔH_m (J g^{-1})
PLA_15PHB	**0**	56.7	124.8	10.7	148	175.8	-	25.1
	1	61.0	123.8	16.6	147.7	175.3	-	30.3
	3	59.0	118.8	19.8	146.5	166.2	-	30
	5	59.7	116.6	20.2	145.8	165.9	-	40
	7	61.0	118.7	13.6	146.3	165.5	-	43.3
PLA_15PHB_30OLA	**0**	35.3	84.6	25.1	145.5	164.4	-	34.4
	1	41.3	-	-	145.9	164.0	177.0	40.3
	3	42.5	-	-	146.2	164.5	177.4	44
	5	43.7	-	-	147.9	165.9	-	64
	7	44.7	-	-	147.6	164.8	-	57.6
PLA_15PHB_30OLA_1CNC	**0**	31.0	88.0	20.4	144,4	160,3	174,4	34.0
	1	41.0	-	-	145.2	163.0	-	35.5
	3	41.1	-	-	146.4	164.9	-	44.8
	5	39.3	-	-	146.5	163.6	-	63.4
	7	38.9	-	-	-	159.5	-	65.4

the end of the seventh day, indicating that no significant hydrolytic degradation and diffusion of water-soluble compounds into the buffer occurs in the test time interval. These results suggest that degradation of films in the presence of Proteinase K could be mainly attributed to the

607 enzyme-catalyzed chain cleavage and the subsequent elution of water-soluble fractions
608 (monomers and low molar mass oligomers) into the buffer medium (Kodama, 2013).

609 It was found that all films developed crystallinity during the first five days of incubation, since
610 the differences between melting and cold crystallization enthalpy values increased with the
611 incubation time (**Table 5**) (Wang, Fan, Hsiue, 2005), with higher increases for plasticized
612 samples. However, no significant effect was observed with the incorporation of 1 wt% CNC in
613 the crystallization process during degradation of the PLA_15PHB_30OLA sample. **Figure 5 c**
614 also shows the disappearance of the cold crystallization peak in PLA_15PHB plasticized samples
615 and the shift of melting peaks to higher temperatures and higher enthalpy values. This increase in
616 crystallinity during enzymatic hydrolysis could be associated to the removal of the short chains
617 in the amorphous regions of the polymer matrix, since Proteinase K preferentially degrades the
618 amorphous domains in the PLA structure (Wang, Fan, Hsiue, 2005; Tsuji & Miyauchi, 2001).
619 The obtained results are in agreement with the increase in the opacity of samples during
620 enzymatic degradation previously discussed. In addition, a slight increase in the T_g values was
621 observed for all materials after one day of incubation, that indicates lower free volume within the
622 polymer network and relatively limited mobility of low molar mass chains. This effect could be
623 attributed to the initial loss of the low molar mass compounds, which are easier to degrade,
624 decreasing the plasticization effect provided by OLA.

625 Finally, surface and fracture morphologies of PLA_15PHB, PLA_PHB_30OLA and
626 PLA_PHB_30OLA_1CNC films were studied by SEM, before and after different times of
627 enzymatic degradation. SEM surface micrographs (**Fig. 5d**) showed that the enzymatic
628 degradation of all samples were appeared in the films surface after three days of incubation,
629 since some erosion and the appearance of cracks and holes were observed. This effect was more

630 evident for plasticized samples, while the PLA_15PHB film showed much smoother surface, in
631 agreement with the weight loss data. These results can be associated with the removal of low
632 molecular weight compounds from the surface substrate by solubilization in the aqueous buffer
633 medium (Tsuji, Echizen, Nishimura, 2006). Micrographs of fracture surfaces for all samples
634 (**Fig. 5e**) after three days of incubation supported the idea that the enzymatic hydrolytic
635 degradation was more relevant in the polymer surface than in the bulk, according to some
636 authors that observed the movement of Proteinase K on the surface to hydrolize PLA films
637 (Yamashita, Kikkawa, Kurokawa & Doi, 2005). It should be noted that no significant differences
638 were observed when CNC were incorporated to the PLA_15PHB_30 OLA formulation in their
639 enzymatic disintegration effects caused on samples morphology after 3 days of test. It can be
640 concluded that all PLA-PHB based films evaluated in this study can be degraded by Proteinase
641 K. The presence of 30 wt % OLA and 1 wt.% CNC can facilitate the enzymatic degradation of
642 the PLA.

643 **4. Conclusion**

644 Biodegradable blends of PLA and PHB plasticized with an oligomer of lactic acid and an
645 antimicrobial natural additive (carvacrol), reinforced with cellulose nanocrystals extracted from
646 microcrystalline cellulose were successfully formulated and extruded to obtain transparent
647 multifunctional films. Mechanical and barrier properties of PLA_15PHB_CNC formulations
648 (CNC content, 1 wt% and 3 wt%) showed good performance, particularly for 1 wt% CNC to
649 enhance the properties of the PLA_15PHB blend. The effect of the addition of a natural
650 plasticizer into this blend was clearly confirmed by the improvement in ductile properties as
651 evaluated by using tensile tests, suggesting the possibility to modulate the use of different
652 components to prepare “tailor-made” blends with properties depending on the final application.

653 The presence of CNC resulted in clear improvement of the barrier properties as a positive effect
654 to the ability of cellulosic reinforcement phase at the nanoscale to increase the tortuous path of
655 gas molecules through the polymer matrix. Specifically, the study of mechanical, barrier and
656 migration characteristics of the PLA_15PHB_15OLA_10Carv_1CNC system underlined the
657 general improvement of properties in these five-components formulations and opened the
658 possibility of their use as films for food packaging. This formulation showed improved elastic
659 modulus and deformation at break with respect to the same blend with no CNC. This behavior
660 was ascribed to the presence of CNC that were able to modulate the mechanical performances in
661 the elastic and plastic regions. Furthermore, as confirmed by FESEM images and DSC analysis,
662 CNC were able to protect carvacrol and OLA during processing, inducing the formation of
663 elliptical shape/lengthened regions, oriented according to the extrusion direction by reducing the
664 glass transition and melting temperatures with respect to PLA_15PHB_15OLA_10Carv. It was
665 concluded that PLA_15PHB_15OLA_10Carv_1CNC nanocomposites will be suitable materials
666 for using as packaging in single-use applications, showing an appropriate balance among
667 barrier, thermal, and mechanical properties.

668 Results on disintegrability under composting conditions and enzymatic degradation using
669 Proteinase K were obtained to evaluate the effect and the influence of different components into
670 the post-use degradation processes. These results showed that all formulations disintegrated in
671 less than 17 days with more than 80 % weight loss. In addition it was observed that the presence
672 of plasticizer promoted the disintegration kinetics. Results of visual, morphological and thermal
673 analysis of samples under enzymatic degradation conditions confirmed that the selected enzyme
674 preferentially degraded amorphous regions and crystallinity of degraded films increased as a

consequence of enzyme action. The proposed innovative approach should be applied at other polymer and/or blend in order to modulate and study different properties.

Funding Sources

This research was financed by the SAMSUNG GRO PROGRAMME 2012.

References

Álvarez-Chávez, C.R., Edwards, S., Moure-Eraso, R. & Geiser, K. (2012). Sustainability of bio-based plastics: general comparative analysis and recommendations for improvement. *Journal of Cleaner Production*, 23, 47–56.

Armentano, I., Bitinis, N., Fortunati, E., Mattioli, S., Rescignano, N., Verdejio, R., Lopez-Manchado M.A., Kenny, J.M. (2013). Multifunctional nanostructured PLA materials for packaging and tissue engineering. *Progress Polymer Science*, 38, 1720–1747.

Armentano, I., Fortunati E., Burgos, N., Dominici, F., Luzi, F., Fiori, S., Jimenez, A., Yoon, K., Ahn, J.; Kang, S.; & Kenny, J.M. (2015). Bio-based PLA_PHB plasticized blend films: Processing and structural characterization. *LWT - Food Science and Technology*, 64, 980–988.

Armentano, I., Fortunati, E., Burgos, N., Dominici, F., Luzi F., Fiori, S., Jimenez, A., Yoon, K., Ahn, J., Kang, S., & Kenny, J.M. (2015) Processing and characterization of plasticized PLA/PHB blends for biodegradable multiphase systems. *eXPRESS Polymer Letters* 9(7), 583-597.

696 Arrieta, M.P., Peltzer, M.A., Lopez, J., Garrigos, M. del Carmen, Valente, A.J.M., Jimenez, A.
697 (2014). Functional properties of sodium and calcium caseinate antimicrobial active films
698 containing carvacrol. *Journal of Food Engineering,* 121, 94–101.

699 Arrieta, M.P., López, J., Rayón, E. & Jiménez, A. (2014). Disintegrability under composting
700 conditions of plasticized PLA–PHB blends. *Polymer Degradation and Stability*, 108, 307–
701 318.

702 Arrieta, M.P., Samper, M.D., Aldas, M. & López, J. (2017) On the Use of PLA-PHB Blends for
703 Sustainable Food Packaging Applications. *Materials* 2017, 10, 1008.

704 Arrieta, M.P., Castro-Lopez, M.del Mar, Rayon, E., Barral-Losada, L.F., et al. (2014).
705 Plasticized Poly(lactic acid)–Poly(hydroxybutyrate) (PLA–PHB) Blends Incorporated with
706 Catechin Intended for Active Food-Packaging Applications. *Journal of Agricultural and*
707 *Food Chemistry* 62, 10170-10180.

708 Arrieta, M.P., Fortunati, E., Dominici, F., López, J. & Kenny, J.M. (2015). Bionanocomposite
709 films based on plasticized PLA–PHB/cellulose nanocrystal blends. *Carbohydrate Polymer*,
710 121, 265–275.

711 Arrieta, M.P., Fortunati, E., Dominici, F., Rayon, E., Lopez, J., Kenny, J.M. (2014).
712 Multifunctional PLA–PHB/cellulose nanocrystal films: Processing, structural and thermal
713 properties. *Carbohydrate Polymer*, 107, 16–24.

714 Arrieta, M.P., Fortunati, E., Dominici, F., Rayon, E., Lopez, J., Kenny, J.M. (2014). PLA-
715 PHB/cellulose based films: Mechanical, barrier and disintegration properties. *Polymer*
716 *Degradation Stability*, 107, 139–149.

717 Arrieta, M.P., López, J., Hernández, A. & Rayón, E. (2014). Ternary PLA–PHB–Limonene
718 blends intended for biodegradable food packaging applications. *European Polymer*
719 *Jou*rnal, 50, 255–270.

720 ASTM E-96/E 96M-05: Standard Test Methods for Water Vapor Transmission of Materials
721 (2005).

722 Atarés, L. & Chiralt, A. (2004) Essential oils as additives in biodegradable films and coatings for
723 active food packaging. *Trends in Food Science & Technology*, 48, 51–62.

724 Boonyawan, D., Sarapirom, S., Tunma, S., Chaiwong, C., Rachtanapun, P., Auras, R. (2011).
725 Characterization and antimicrobial properties of fluorine-rich carbon films deposited on
726 poly(lactic acid). *Surface and Coating Technology*, 205, S552–S557.

727 Burgos, N., Armentano, I., Fortunati, E., Dominici, F., Luzi, F., Fiori, S., Cristofaro, F., Visai,
728 L., Jimenez, A., Kenny, J.M. (2017). Functional Properties of Plasticized Bio-Based
729 Poly(Lactic Acid)_Poly(Hydroxybutyrate) (PLA_PHB) Films for Active Food Packaging.
730 *Food Bioprocess Technology*, 10, 770–780.

731 Burgos, N., Tolaguera, D., Fiori, S., Jimenez, A. (2013). Synthesis and Characterization of
732 Lactic Acid Oligomers: Evaluation of Performance as Poly(Lactic Acid) Plasticizers.
733 *Journal of Polymers and the Environment*, 22, 227-235.

734 Burgos, N., Martino, V.P. & Jiménez, A. (2013). Characterization and ageing study of
735 poly(lactic acid) films plasticized with oligomeric lactic acid. *Polymer Degradation and*
736 *Stability*, 98, 651–658.

737 Cano, A.I., Cháfer, M., Chiralt, A. & González-Martínez, C. (2015). Physical and
738 microstructural properties of biodegradable films based on pea starch and PVA. *Journal of Food*
739 *Engineering*, 167, 59–64.

740 Commission Regulation EU Nº 10/2011 on plastic materials and articles intended to come into
741 contact with food. Official Journal of European Communities (2011).

742 Cranston, E.D. & Gray, D.G. (2006) Morphological and Optical Characterization of
743 Polyelectrolyte Multilayers Incorporating Nanocrystalline Cellulose. *Biomacromolecules*,
744 7, 2522–2530.

745 Dhar, P., Bhardwaj, U., Kumar, A. & Katiyar, V. (2015).Poly (3-hydroxybutyrate)/cellulose
746 nanocrystal films for food packaging applications: Barrier and migration studies. Polymer
747 Engineering & Science, 55, 2388–2395.

748 Fortunati, E., Peltzer, M., Armentano, I., Torre, L., Jimenez, A., and Kenny, J.M. (2012) Effects
749 of modified cellulose nanocrystals on the barrier and migration properties of PLA nano-
750 biocomposites. *Carbohydrate Polymers* 2012, 90, 948–956.

751 Fortunati, E., Gigli, M., Luzi, F., Dominici, F., Lotti, N., Gazzano, M., Cano, A., Chiralt, A.,
752 Munari, A. Kenny, J.M., Armentano, I., Torre, L. (2017) Processing and characterization
753 of nanocomposite based on poly(butylene/triethylene succinate) copolymers and cellulose
754 nanocrystals. *Carbohydrate Polymers*, 165, 51–60.

755 Fortunati, E., Luzi, F., Puglia, D., Dominici, F., Santulli, C., Kenny, J.M., Torre, L. (2014)
756 Investigation of thermo-mechanical, chemical and degradative properties of PLA-limonene

757 films reinforced with cellulose nanocrystals extracted from Phormium tenax leaves.
758 *European Polymer Journal*, 56, 77–91.

759 Fortunati, E., Puglia, D., Luzi, F., Santulli, C., Kenny, J.M., Torre, L. (2013). Binary PVA bio-
760 nanocomposites containing cellulose nanocrystals extracted from different natural sources:
761 Part I. *Carbohydrate Polymers,* 97, 825–836.

762 Habibi, Y., Aouadi, S., Raquez, J.M. & Dubois, P. (2013). Effects of interfacial
763 stereocomplexation in cellulose nanocrystal-filled polylactide nanocomposites. *Cellulose*,
764 20, 2877–2885.

765 ISO20200 - Determination of the degree of disintegration of plastic materials under simulated
766 composting conditions in a laboratory-scale test.

767 Kodama, Y. (2013) Degradability: Enzymatic and in Simulated Compost Soil of PLLA:PCL
768 Blend and on Their Composite with Coconut Fiber. Chapter six in Biodegradation of
769 Hazardous and Special Product. doi:10.5772/56231

770 Luzi, F., Fortunati, E., Jimenez, J., Puglia, D., Pezzolla, D., Gigliotti, G., Kenny, J.M., Chiralt,
771 A., Torre, L. (2016). Production and characterization of PLA_PBS biodegradable blends
772 reinforced with cellulose nanocrystals extracted from hemp fibres. *Industrial Crops and*
773 *Products. Nanocellulose Prod. Funct. Appl.,* 93, 276–289.

774 Luzi, F., Fortunati, E., Puglia, D., Lavorgna, M., Santulli, C., Kenny, J.M., Torre, L. (2014)
775 Optimized extraction of cellulose nanocrystals from pristine and carded hemp fibres.
776 *Industrial Crops and Products*, 56, 175–186.

Luzi, F., Fortunati, E., Puglia, D., Petrucci, R., Kenny, J.M., Torre, L. (2015). Study of disintegrability in compost and enzymatic degradation of PLA and PLA nanocomposites reinforced with cellulose nanocrystals extracted from Posidonia Oceanica. *Polymer Degradation and Stability*, 121, 105–115.

Luzi, F., Fortunati, E., Puglia, D., Petrucci, R., Kenny, J.M., Torre, L. (2016). Modulation of Acid Hydrolysis Reaction Time for the Extraction of Cellulose Nanocrystals from Posidonia oceanica Leaves. *Journal of Renewable Materials*, 4, 190-198.

Martino, V.P., Jiménez, A., Ruseckaite, R.A. & Avérous, L. (2011). Structure and properties of clay nano-biocomposites based on poly(lactic acid) plasticized with polyadipates. *Polymer for Advanced Technologies*, 22, 2206–2213.

Mlalila, N., Hilonga, A., Swai, H., Devlieghere, F. & Ragaert, P. (2018). Antimicrobial packaging based on starch, poly(3-hydroxybutyrate) and poly(lactic-co-glycolide) materials and application challenges. *Trends in Food Science & Technology*, 74, 1–11.

Nostro, A. & Papalia, T. (2012). Antimicrobial Activity of Carvacrol: Current Progress and Future Prospectives. *Recent Patents on Anti-Infective Drug Discovery*, 7, 28-35.

Ruiz, M.M., Cavaillé, J.Y., Dufresne, A., Gérard, J.F. & Graillat, C. (2000). Processing and characterization of new thermoset nanocomposites based on cellulose whiskers. *Composite Interfaces*, 7, 117–131.

Sanchez-Garcia, M.D. & Lagaron, J.M. (2010). On the use of plant cellulose nanowhiskers to enhance the barrier properties of polylactic acid. *Cellulose*, 17, 987–1004.

797 Seoane, I.T., Cerrutti,P., Vazquez, A.; Cyras, V.P.; Manfredi, L.B. (2019). Ternary
798 nanocomposites based on plasticized poly(3- hydroxybutyrate) and nanocellulose.
799 *Polymer Bulletin*, 76:967–988.

800 Shi, Q., Zhou, C., Yue, Y., Guo, W., Wu, Y., Wu, Q. (2012). Mechanical properties and in vitro
801 degradation of electrospun bio-nanocomposite mats from PLA and cellulose nanocrystals.
802 *Carbohydrate Polymers*, 90, 301-308.

803 Tsuji, H. & Miyauchi, S. Poly(l-lactide): (2001). 7. Enzymatic hydrolysis of free and restricted
804 amorphous regions in poly(l-lactide) films with different crystallinities and a fixed
805 crystalline thickness. *Polymer*, 42, 4463–4467.

806 Tsuji, H., Echizen, Y. & Nishimura, Y. (2006). Enzymatic Degradation of Poly(l-Lactic Acid):
807 Effects of UV Irradiation. *Journal of Polymer and Environment*, 14, 239–248.

808 Valdés, A., Mellinas, A.C., Ramos, M., Garrigós, M.C. & Jiménez, A. (2014). Natural additives
809 and agricultural wastes in biopolymer formulations for food packaging. *Frontiers in*
810 *Chemistry*, 2.

811 Wang, C.H., Fan, K.R., Hsiue, G.H. (2005). Enzymatic degradation of PLLA-PEOz-PLLA
812 triblock copolymers. *Biomaterials*, 26, 2803-2811.

813 Yamashita, K., Kikkawa, Y., Kurokawa, K., & Doi, Y. (2005). Enzymatic Degradation of Poly(l-
814 lactide) Film by Proteinase K: Quartz Crystal Microbalance and Atomic Force Microscopy
815 Study. *Biomacromolecules*, 6, 850-857.

816 Youssef, A.M. & El-Sayed, S.M. (2018). Bionanocomposites materials for food packaging
817 applications: Concepts and future outlook. *Carbohydrate Polymers*, 193, 19–27.

818 Zhang, M. & Thomas, N.L. (2011). Blending polylactic acid with polyhydroxybutyrate: The
819 effect on thermal, mechanical, and biodegradation properties. *Advances in Polymer*
820 *Technology*, 30, 67–79.

821 Zhao, Z., Yang, L., Hua, J., Wei, J., Gachet, S., El Ghzaoui, Li, S. (2008). Relationship between
822 Enzyme Adsorption and Enzyme-Catalyzed Degradation of Polylactides. *Macromolecular*
823 *Bioscience*, 8, 25–31.

824 Zhu, L., Zhong, L., Wu, X., Li, M., Wang, H., You, J., & Li, C. (2018). Shapeable Fibrous
825 Aerogels of Metal–Organic-Frameworks Templated with Nanocellulose for Rapid and